Adaptive Fuzzy Strong Tracking Extended Kalman Filtering for GPS Navigation

Dah-Jing Jwo and Sheng-Hung Wang

***Abstract*—The well-known extended Kalman filter (EKF) has been widely applied to the Global Positioning System (GPS) navigation processing. The adaptive algorithm has been one of the approaches to prevent the divergence problem of the EKF when precise knowledge on the system models are not available. One of the adaptive methods is called the strong tracking Kalman filter (STKF), which is essentially a nonlinear smoother algorithm that employs suboptimal multiple fading factors, in which the softening factors are involved. Traditional approach for selecting the softening factors heavily relies on personal experience or computer simulation. In order to resolve this shortcoming, a novel scheme called the adaptive fuzzy strong tracking Kalman filter (AFSTKF) is carried out. In the AFSTKF, the fuzzy logic reasoning system based on the Takagi–Sugeno (T-S) model is incorporated into the STKF. By monitoring the degree of divergence (DOD) parameters based on the innovation information, the fuzzy logic adaptive system (FLAS) is designed for dynamically adjusting the softening factor according to the change in vehicle dynamics. GPS navigation processing using the AFSTKF will be simulated to validate the effectiveness of the proposed strategy. The performance of the proposed scheme will be assessed and compared with those of conventional EKF and STKF.**

***Index Terms*—Adaptive extended Kalman filtering, fuzzy logic adaptive system (FLAS), global positioning system (GPS), strong tracking Kalman filter (STKF).**

I. Introduction

The Global Positioning System (GPS) is a satellite-based navigation system that provides a user with the proper equipment access to useful and accurate positioning information anywhere on the globe. The well-known Kalman filter [1]–[3], which provides optimal (minimum mean-square error) estimate of the system state vector, has been widely applied to the fields of navigation such as GPS receiver position/velocity determination.

While employed in the GPS receiver [3] as the navigational state estimator, the extended Kalman filter (EKF) has been one of the promising approaches. To obtain good estimation solutions using the EKF approach, the designers are required to have good knowledge on both dynamic process (plant dynamics, using an estimated internal model of the dynamics of the system) and measurement models, in addition to the assumption that both the process and measurement are corrupted by zero-mean white noises. The divergence due to modeling errors is a critical problem in Kalman filter applications. If the theoretical behavior of a filter and its actual behavior do not agree, divergence may occur. A conventional Kalman filter fails to ensure error convergence due to limited knowledge of the system's dynamic model and measurement noise. If the Kalman filter is provided with information that the process behaves a certain way, whereas, in fact, it behaves a different way, the filter will continually intend to fit an incorrect process signal.

In the Kalman filter, the system model, system initial conditions, and noise characteristics have to be specified *a priori*. In various circumstances, there are uncertainties in the system models and noise description, and the assumptions on the statistics of disturbances are violated since in a number of practical situations, the availability of a precisely known model is unrealistic. The facts discussed above results in filtering performance degradation. In actual navigation filter designs, there exist model uncertainties which cannot be expressed by the linear state-space model. The linear model increases modeling errors since the actual vehicle motions are nonlinear process. Very often, it is the case that little *a priori* knowledge is available concerning the maneuver. Hence, compensation of the uncertainties is an important task in the navigation filter design. In the modeling strategy, some phenomena are disregarded and a way to take them into account is to consider a nominal model affected by uncertainty.

To prevent divergence problems due to modeling errors using the EKF approach, the adaptive filter algorithm has been one of the strategies considered for estimating the state vector. Many efforts have been made to improve the estimation of the covariance matrices. Mehra [4] classified the adaptive approaches into four categories: Bayesian, maximum-likelihood, correlation, and covariance matching. These methods can be applied to the Kalman filtering algorithm for realizing the adaptive Kalman filtering [4], [5]. However, the first two methods are computationally demanding so that their practical applications are limited. As for the correlation methods, a set of equations is derived to relate the functions to the unknown parameter. The covariance matching technique attempts to make the filter residuals consistent with their theoretical covariances. One of the methods proposed is called the strong tracking Kalman filter (STKF) [6], [7]. The STKF is essentially a nonlinear smoother algorithm that employs suboptimal multiple fading factors, in which the softening factors are involved. STKF has several merits, such as: 1) strong robustness against model uncertainties and 2) good real-time state tracking ability even

Manuscript received June 15, 2006; revised October 20, 2006; accepted October 22, 2006. This work was supported in part by the National Science Council of the Republic of China under Grant NSC 94-2212-E-019-003. The associate editor coordinating the review of this paper and approving it for publication was Dr. Gourab Sen Gupta.

The authors are with the Department of Communications and Guidance Engineering, National Taiwan Ocean University, Keelung 202-24, Taiwan, R.O.C. (e-mail: djjwo@mail.ntou.edu.tw; u8370247@tknet.tku.edu.tw).

Color versions of one or more of the figures in this paper are available online at http://ieeexplore.ieee.org.

Digital Object Identifier 10.1109/JSEN.2007.894148

when a state jump occurs, no matter whether the system has reached steady state or not.

The application of fuzzy logic [8] to adaptive Kalman filtering has been becoming popular, e.g., [9]–[12]. Sasiadek *et al.* introduced the Fuzzy Logic Adaptive System (FLAS) for adapting the process and measurement noise covariance matrices in navigation data fusion design [9]. Abdelnour *et al.* used the exponential-weighting algorithm for detecting and correcting the divergence of the Kalman filter [10]. Kobayashi *et al.* proposed a method for generating an accurate estimate of the absolute speed of a vehicle from noisy acceleration and erroneous wheel speed information [11]. The method employed the fuzzy logic rule-based Kalman filter to handle abrupt wheel skid and slip, and poor signal-to-noise sensor data. Mostov and Soloviev proposed the method to increase the Kalman filter order, which in turn enhances the accuracy of smoothing and thus location finding for kinematic GPS [12].

In a STKF, the softening factor is introduced to provide better state estimation smoothness. Traditional STKF approach for determining the softening factors heavily relies on personal experience or computer simulation using a heuristic searching scheme. In order to resolve this shortcoming, a new approach called the adaptive fuzzy strong tracking Kalman filter (AFSTKF) is proposed. The fuzzy logic reasoning system based on the Takagi–Sugeno (T-S) model is incorporated into the STKF for real-time for tuning the softening factor. Instead of determining the fading factor directly, determining the softening factor provides the alternative design strategy based on the theory of STKF, for which the convergence has been ensured. The fuzzy reasoning system is constructed for obtaining suitable softening factors according to the time-varying change in dynamics. By monitoring the innovation information, the FLAS is employed for dynamically adjusting the softening factors based on the proposed fuzzy rule. Using the AFSTKF, the FLAS, which is the filter's internal mode, is used to continually adjust the softening factor so as to improve the Kalman filter performance.

This paper is organized as follows. In Section II, preliminary background on GPS navigation processing is reviewed. The proposed strategy of the AFSTKF approach is introduced in Section III. Several parameters for determining the degree of divergence (DOD) are introduced for identifying the degree of change in vehicle dynamics based on the innovation information. In Section IV, simulation experiments on GPS navigation processing are carried out to evaluate the performance of the approach in comparison to those by conventional EKF and STKF. Conclusions are given in Section V.

II. GPS Navigation Processing

The most commonly used approaches for the GPS navigation solutions [2], [3] are the least squares [3] and the extended Kalman filtering approaches [1], [2]. The Kalman filter is briefly reviewed for convenience.

A. Linearization of GPS Pseudorange Equations

Consider the vectors relating the Earth's center, satellites, and user position. The vector $\mathbf{s}$ represents the vector from the Earth's center to a satellite, $\mathbf{u}$ represents the vector from the Earth's center to the user's position, and $\mathbf{r}$ represents the vector from the user to satellite, we can write the vector relation

$$\mathbf{r} = \mathbf{s} - \mathbf{u}. \tag{1}$$

The distance $\|\mathbf{r}\|$ is computed by measuring the propagation time from the transmitting satellite to the user/receiver. The pseudorange ρ_i is defined for the ith satellite by

$$\rho_i = \|\mathbf{s}_i - \mathbf{u}\| + ct_b + v_{\rho_i} \tag{2}$$

where c is the speed of light and t_b is the receiver clock offset from system time, and v_{ρ_i} is the pseudorange measurement noise. Consider the user position in three dimensions, denoted by (x_u, y_u, z_u), the GPS pseudorange measurements made to the n satellites can then be written as

$$\rho_i = \sqrt{(x_i - x_u)^2 + (y_i - y_u)^2 + (z_i - z_u)^2} + ct_b + v_{\rho_i}, \quad i = 1, \ldots, n \tag{3}$$

where (x_i, y_i, z_i) denotes the ith satellite's position in three dimensions.

The states and the measurements are related nonlinearly; the nonlinear ranges are linearized around an operating point using Taylor's series. Equation (3) can be linearized by expanding Taylor's series around the approximate (or nominal) user position $(\hat{x}_n, \hat{y}_n, \hat{z}_n)$ and neglecting the higher terms. Defining $\hat{\rho}_i$ as ρ_i at $(\hat{x}_n, \hat{y}_n, \hat{z}_n)$ gives

$$\Delta\rho_i = \rho_i - \hat{\rho}_i = e_{i1}\Delta x_u + e_{i2}\Delta y_u + e_{i3}\Delta z_u + ct_b + v_{\rho_i} \tag{4}$$

where

$$e_{i1} = \frac{\hat{x}_n - x_i}{\hat{r}_i}; \quad e_{i2} = \frac{\hat{y}_n - y_i}{\hat{r}_i}; \quad e_{i3} = \frac{\hat{z}_n - z_i}{\hat{r}_i}$$
$$\hat{r}_i = \sqrt{(\hat{x}_n - x_i)^2 + (\hat{y}_n - y_i)^2 + (\hat{z}_n - z_i)^2}. \tag{5}$$

The vector $(e_{i1}, e_{i2}, e_{i3}) \equiv \mathbf{E}_i, i = 1, \ldots, n$, denotes the line-of-sight vector from the user to the satellites. Equation (4) can be written in a matrix formulation

$$\Delta\rho_i = [\,\Delta\rho_1 \quad \Delta\rho_2 \quad \Delta\rho_3 \quad \cdots \quad \Delta\rho_n\,]^T = \begin{bmatrix} e_{11} & e_{12} & e_{13} & 1 \\ e_{21} & e_{22} & e_{23} & 1 \\ e_{31} & e_{32} & e_{33} & 1 \\ \vdots & \vdots & \vdots & \vdots \\ e_{n1} & e_{n2} & e_{n3} & 1 \end{bmatrix} \begin{bmatrix} \Delta x_u \\ \Delta y_u \\ \Delta z_u \\ ct_b \end{bmatrix} + v_{\rho_i} \tag{6}$$

which can be represented as

$$\mathbf{z} = \mathbf{B}\mathbf{x} + \mathbf{v}. \tag{7}$$

The dimension of matrix $\mathbf{B}$ is $n \times 4$ with $n \geqslant 4$, and $\mathbf{B}$ is usually referred to as the "geometry matrix" or "visibility matrix." The least squares solution to (7) is given by

$$\hat{\mathbf{x}} = (\mathbf{B}^{\mathrm{T}}\mathbf{B})^{-1}\mathbf{B}^{\mathrm{T}}\mathbf{z}. \tag{8}$$

B. GPS Navigation Processing Using the Extended Kalman Filter (EKF)

Kalman filtering has been recognised as one of the most powerful state estimation techniques. The purpose of the Kalman filter is to provide the estimation with minimum error variance. The EKF is a nonlinear version of the Kalman filter and is widely used for the position estimation in GPS receivers. A superior way of solving the GPS equations is to use the EKF.

The process model and measurement model for the Kalman filter are represented as

$$\text{Process model}: \dot{\mathbf{x}} = \mathbf{F}\mathbf{x} + \mathbf{G}\mathbf{u} \tag{9a}$$

$$\text{Measurement model}: \mathbf{z} = \mathbf{H}\mathbf{x} + \mathbf{v} \tag{9b}$$

where the vectors $\mathbf{u}(t)$ and $\mathbf{v}(t)$ are both white noise sequences with zero means and mutually independent

$$E[\mathbf{u}(t)\mathbf{u}^{\mathrm{T}}(\tau)] = q\delta(t-\tau); \quad E[\mathbf{v}(t)\mathbf{v}^{\mathrm{T}}(\tau)] = r\delta(t-\tau);$$
$$E[\mathbf{u}(t)\mathbf{v}^{\mathrm{T}}(\tau)] = \mathbf{0} \tag{10}$$

where $\delta(t)$ is the Dirac delta function, $E[\cdot]$ represents expectation, and superscript "T" denotes matrix transpose.

Expressing (9a) and (9b) in discrete-time equivalent form leads to

$$\mathbf{x}_{k+1} = \mathbf{\Phi}_k \mathbf{x}_k + \mathbf{w}_k \tag{11a}$$

$$\mathbf{z}_k = \mathbf{H}_k \mathbf{x}_k + \mathbf{v}_k \tag{11b}$$

where the state vector $\mathbf{x}_k \in \Re^n$, process noise vector $\mathbf{w}_k \in \Re^n$, measurement vector $\mathbf{z}_k \in \Re^m$, and measurement noise vector $\mathbf{v}_k \in \Re^m$. In (11), both the vectors $\mathbf{w}_k$ and $\mathbf{v}_k$ are zero-mean Gaussian white sequences having zero cross correlation with each other

$$\mathbf{E}\left[\mathbf{w}_k\mathbf{w}_i^{\mathrm{T}}\right] = \begin{cases} \mathbf{Q}_k, & i = k \\ 0, & i \neq k \end{cases};$$
$$\mathbf{E}\left[\mathbf{v}_k\mathbf{v}_i^{\mathrm{T}}\right] = \begin{cases} \mathbf{R}_k, & i = k \\ 0, & i \neq k \end{cases};$$
$$\mathbf{E}\left[\mathbf{w}_k\mathbf{v}_i^{\mathrm{T}}\right] = \mathbf{0}, \quad \text{for all } i \text{ and } k \tag{12}$$

where $\mathbf{Q}_k$ is the process noise covariance matrix, $\mathbf{R}_k$ is the measurement noise covariance matrix, $\mathbf{\Phi}_k = e^{\mathbf{F}\Delta t}$ is the state transition matrix, and Δt is the sampling interval.

The discrete-time Kalman filter algorithm is summarized as follows.

Prediction steps/time update equations

$$\hat{\mathbf{x}}_{k+1}^- = \mathbf{\Phi}_k \hat{\mathbf{x}}_k \tag{13}$$

$$\mathbf{P}_{k+1}^- = \mathbf{\Phi}_k \mathbf{P}_k \mathbf{\Phi}_k^{\mathrm{T}} + \mathbf{Q}_k. \tag{14}$$

Correction steps/measurement update equations

$$\mathbf{K}_k = \mathbf{P}_k^- \mathbf{H}_k^{\mathrm{T}} \left[\mathbf{H}_k \mathbf{P}_k^- \mathbf{H}_k^{\mathrm{T}} + \mathbf{R}_k\right]^{-1} \tag{15}$$

$$\hat{\mathbf{x}}_k = \hat{\mathbf{x}}_k^- + \mathbf{K}_k[\mathbf{z}_k - \mathbf{H}_k\hat{\mathbf{x}}_k^-] \tag{16}$$

$$\mathbf{P}_k = [\mathbf{I} - \mathbf{K}_k\mathbf{H}_k]\mathbf{P}_k^-. \tag{17}$$

Equations (13)–(14) are the time update equations of the algorithm from k to step $k+1$, and (15)–(17) are the measurement update equations. These equations incorporate a measurement value into *a priori* estimation to obtain an improved *a posteriori* estimation. In the above equations, $\mathbf{P}_k$ is the error covariance matrix defined by $E[(\mathbf{x}_k - \hat{\mathbf{x}}_k)(\mathbf{x}_k - \hat{\mathbf{x}}_k)^{\mathrm{T}}]$, in which $\hat{\mathbf{x}}_k$ is an estimation of the system state vector $\mathbf{x}_k$, and the weighting matrix $\mathbf{K}_k$ is generally referred to as the Kalman gain matrix. The Kalman filter algorithm starts with an initial condition value, $\hat{\mathbf{x}}_0^-$ and $\mathbf{P}_0^-$. When new measurement $\mathbf{z}_k$ becomes available with the progression of time, the estimation of states and the corresponding error covariance would follow recursively ad infinity.

The extended Kalman filtering is a nonlinear version of Kalman filtering, which deals with the case described by the nonlinear stochastic differential equations

$$\dot{\mathbf{x}} = \mathbf{f}(\mathbf{x}, t) + \mathbf{u}(t) \tag{18a}$$

$$\mathbf{z} = \mathbf{h}(\mathbf{x}, t) + \mathbf{v}(t). \tag{18b}$$

The algorithm for the extended Kalman filtering is essentially similar to that of Kalman filtering, except that some modifications are made. First, the state update equation becomes

$$\hat{\mathbf{x}}_k = \hat{\mathbf{x}}_k^- + \mathbf{K}_k[\mathbf{z}_k - \hat{\mathbf{z}}_k^-] \tag{19}$$

where

$$\hat{\mathbf{x}}_k^- = \mathbf{f}_{k-1}(\hat{\mathbf{x}}_{k-1}) \tag{20a}$$

and

$$\hat{\mathbf{z}}_k^- = \mathbf{h}_k(\hat{\mathbf{x}}_k^-). \tag{20b}$$

Second, the linear approximation equations for system and measurement matrices are obtained through the relations

$$\mathbf{\Phi}_k \approx \left.\frac{\partial \mathbf{f}_k}{\partial \mathbf{x}}\right|_{\mathbf{x}=\hat{\mathbf{x}}_k^-}; \quad \mathbf{H}_k \approx \left.\frac{\partial \mathbf{h}_k}{\partial \mathbf{x}}\right|_{\mathbf{x}=\hat{\mathbf{x}}_k^-}. \tag{21}$$

Further detailed discussion can be referred to Gelb [1] and Brown and Hwang [2]. The flow chart for the GPS navigation processing using EKF approach is shown in Fig. 1.

III. The Adaptive Fuzzy Strong Tracking Kalman Filter (AFSTKF)

The implementation of Kalman filter requires the *a priori* knowledge of both the process and measurement models. Poor knowledge of the models may seriously degrade the Kalman filter performance, and even provoke the filter divergence. To fulfil the requirement, an adaptive Kalman filter can be utilized as the noise-adaptive filter to adjust the parameters.

Mehra [4] classified the adaptive approaches into four categories: Bayesian, maximum-likelihood, correlation, and covariance matching. The innovation sequences have been utilized by the correlation and covariance-matching techniques to estimate the noise covariances. The basic idea behind the covariance-matching approach is to make the actual value of the covariance of the residual consistent with its theoretical value. From the incoming measurement $\mathbf{z}_k$ and the optimal prediction $\hat{\mathbf{x}}_k^-$ obtained in the previous step, the innovation sequence is defined as

$$\boldsymbol{\upsilon}_k = \mathbf{z}_k - \hat{\mathbf{z}}_k^-. \tag{22}$$

The innovation represents the additional information available to the filter as a consequence of the new observation $\mathbf{z}_k$. The

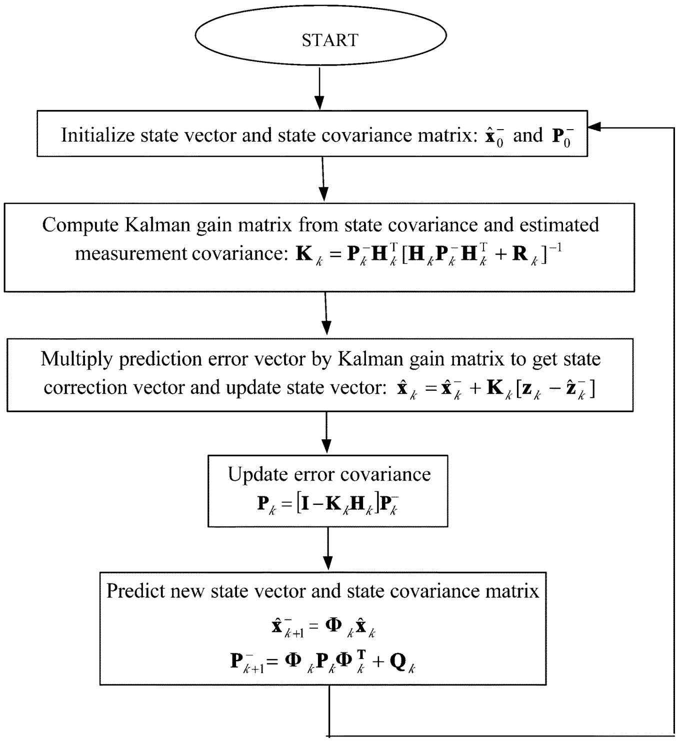

Fig. 1. Flow chart for the GPS Kalman filter.

weighted innovation, $\mathbf{K}_k(\mathbf{z}_k - \hat{\mathbf{z}}_k^-)$, acts as a correction to the predicted estimate $\hat{\mathbf{x}}_k^-$ to form the estimation $\hat{\mathbf{x}}_k$.

One of the approaches for adaptive processing is on the incorporation of fading factors. The idea of fading memory is to apply a factor matrix to the predicted covariance matrix to deliberately increase the variance of the predicted state vector

$$\mathbf{P}_{k+1}^- = \boldsymbol{\lambda}_k\mathbf{\Phi}_k\mathbf{P}_k\mathbf{\Phi}_k^T + \mathbf{Q}_k \tag{23}$$

where $\boldsymbol{\lambda}_k = \mathrm{diag}(\lambda_1, \lambda_2 \ldots, \lambda_m)$. The main difference between different fading memory algorithms is on the calculation of scale factor matrix $\boldsymbol{\lambda}_k$. One approach is to assign the scale factors as constants. When $\lambda_i \leqslant 1$ $(i = 1, 2, \ldots, m)$, the filtering is in a steady-state processing while $\lambda_i > 1$, the filtering may tend to be unstable. For the case $\lambda_i = 1$, it deteriorates to the standard Kalman filter. There are some drawbacks with constant factors, e.g., as the filtering proceeds, the precision of the filtering will decrease because the effects of old data tend to become less and less. The ideal way is to use time-varying factors that are determined according to the dynamic and observation model accuracy.

A. Strong Tracking Kalman Filter (STKF)

It is well known that the process model is dependent on the dynamical characteristics of the vehicle onto which the navigation system is placed. In order to overcome the defect of the conventional Kalman filtering, Zhou *et al.* [6] proposed a concept of STKF and solved the state estimation problem of a class of nonlinear systems with white noise. In the so-called STKF algorithm, suboptimal fading factors are introduced into the nonlinear smoother algorithm. The STKF has several important merits including: 1) strong robustness against model uncertainties and 2) good real-time state tracking capability even when a state jump occurs, no matter whether the system has reached steady state or not. Zhou *et al.* proved that a filter is called the STKF only if the filter satisfies the orthogonal principle stated as follows.

Orthogonal Principle: The sufficient condition for a filter to be called the STKF is only if the time-varying filter gain matrix is selected online such that the state estimation mean-square error is minimized and the innovations remain orthogonal [6]

$$\begin{aligned} &E[\mathbf{x}_k - \hat{\mathbf{x}}_k][\mathbf{x}_k - \hat{\mathbf{x}}_k]^T = \min \\ &E[\boldsymbol{v}_{k+j}\boldsymbol{v}_k^T] = 0, \quad k = 0, 1, 2 \ldots, \quad j = 1, 2 \ldots \end{aligned} \tag{24}$$

Equation (24) is required for ensuring that the innovation sequence will be remained orthogonal. The time-varying suboptimal scaling factor is incorporated, for online tuning the covariance of the predicted state, which adjusts the filter gain, and accordingly the STKF is developed. The suboptimal scaling factor in the time-varying filter gain matrix is given by

$$\lambda_{i,k} = \begin{cases} \alpha_i c_k, & \alpha_i c_k \geqslant 1 \\ 1, & \alpha_i c_k < 1 \end{cases} \tag{25}$$

where

$$c_k = \frac{\mathrm{tr}[\mathbf{N}_k]}{\mathrm{tr}[\boldsymbol{\alpha}\mathbf{M}_k]} \tag{26}$$

and

$$\mathbf{N}_k = \mathbf{V}_k - \beta\mathbf{R}_k - \mathbf{H}_k\mathbf{Q}_k\mathbf{H}_k^T \tag{27a}$$

$$\mathbf{M}_k = \mathbf{H}_k\mathbf{\Phi}_k\mathbf{P}_k\mathbf{\Phi}_k^T\mathbf{H}_k^T \tag{28}$$

$$\mathbf{V}_k = \begin{cases} \boldsymbol{v}_0\boldsymbol{v}_0^T, & k = 0 \\ \frac{[\rho\mathbf{V}_{k-1} + \boldsymbol{v}_k\boldsymbol{v}_k^T]}{1+\rho}, & k \geqslant 1 \end{cases}. \tag{29}$$

The predicted covariance matrix is represented by (23): $\mathbf{P}_{k+1}^- = \boldsymbol{\lambda}_k\mathbf{\Phi}_k\mathbf{P}_k\mathbf{\Phi}_k^T + \mathbf{Q}_k$, where the variables $\mathbf{H}_k, \mathbf{\Phi}_k, \mathbf{Q}_k$, and $\mathbf{R}_k$ are as defined in Section II-B. Equation (27a) can be modified by multiplying an additional parameter $\boldsymbol{\gamma}$, which can be a scalar of a diagonal matrix

$$\mathbf{N}_k = \boldsymbol{\gamma}\mathbf{V}_k - \beta\mathbf{R}_k - \mathbf{H}_k\mathbf{Q}_k\mathbf{H}_k^T. \tag{27b}$$

This parameter is introduced for increasing the tracking capability through the increase of covariance matrix of the innovation.

The key parameter in the STKF is the fading factor matrix $\boldsymbol{\lambda}_k$, which is dependent on three parameters including: 1) α_i; 2) the forgetting factor (ρ); and 3) the softening factor (β). These parameters are usually selected empirically. $\alpha_i \geqslant 1, i = 1, 2, \ldots, m$, which are *a priori* selected. If from *a priori* knowledge, we have the knowledge that $\mathbf{x}$ will have a large change, then a large α_i should be used so as to improve the tracking capability of the STKF. On the other hand, if no *a priori* knowledge about the plant dynamic, it commonly selects $\alpha_1 = \alpha_2 = \cdots = \alpha_m = 1$. In such a case, the STKF based on multiple fading factors deteriorates to a STKF based on a single fading factor. The range of the forgetting factor is $0 < \rho \leqslant 1$, for which 0.95 is commonly used. The softening factor β is utilized to improve the smoothness of state estimation. A larger β (with value no less than 1) leads to better estimation accu-

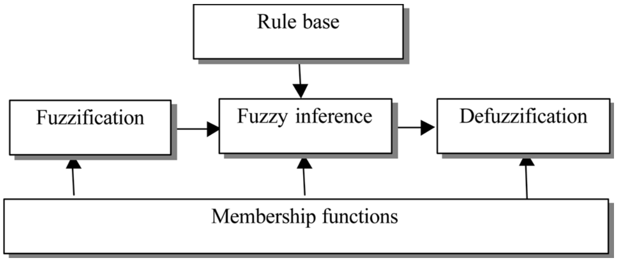

Fig. 2. A fuzzy system.

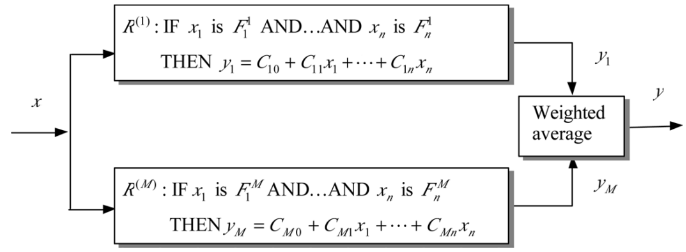

Fig. 3. T-S fuzzy system.

racy, while a smaller β provides stronger tracking capability. The value is usually determined empirically through computer simulation and $\beta = 4.5$ is a commonly selected value.

B. The Fuzzy Logic Adaptive System (FLAS)

Fuzzy logic was first developed by Zadeh in the mid-1960s for representing uncertain and imprecise knowledge. It provides an approximate but effective means of describing the behavior of systems that are too complex, ill-defined, or not easily analyzed mathematically. A typical fuzzy system consists of three components, that is, fuzzification, fuzzy reasoning (fuzzy inference), and fuzzy defuzzification, as shown in Fig. 2. The fuzzification process converts a crisp input value to a fuzzy value, the fuzzy inference is responsible for drawing calculations from the knowledge base, and the fuzzy defuzzification process converts the fuzzy actions into a crisp action.

The fuzzification modules: 1) transforms the error signal into a normalized fuzzy subset consisting of a subset for the range of the input values and a normalized membership function describing the degree of confidence of the input belonging to this range and 2) selects reasonable and good, ideally optimal, membership functions under certain convenient criteria meaningful to the application. The characteristics of the fuzzy adaptive system depend on the fuzzy rules and the effectiveness of the rules directly influences its performance. To obtain the best deterministic output from a fuzzy output subset, a procedure for its interpretation, known as defuzzification should be considered. The defuzzification is used to provide the deterministic values of a membership function for the output. Using fuzzy logic to infer the consequent of a set of fuzzy production rules invariably leads to fuzzy output subsets.

Fuzzy modeling is the method of describing the characteristics of a system using fuzzy inference rules. In this paper, a T-S fuzzy system is used to detect the divergence of EKF and adapt the filter. Takagi and Sugeno proposed a fuzzy modeling approach to model nonlinear systems. The T-S fuzzy system represents the conclusion by functions. The typical T-S system is shown in Fig. 3.

A typical rule in the T-S model has the form:

IF Input x_1 is F_1^1 and Input x_2 is F_2^1 ... and Input x_n is F_n^1 THEN Output $y_k = f_k(x_1, x_2, \ldots, x_n) = C_{k0} + C_{k1}x_1 + \cdots + C_{kn}x_n$.

where $C_{ki}(i = 0 \sim n)$ are constants in the kth rule. For the first-order model, we have the rule in the form:

IF Input x_1 is F_1^1 and Input x_2 is F_2^1 THEN Output $y_k = C_{10} + C_{11}x_1 + C_{12}x_2$.

where F_1^1 and F_2^1 are fuzzy sets and C_{10}, C_{11}, and C_{12} are constants. For a zero-order model, the output level is a constant:

IF Input x_1 is F_1^1 and Input x_2 is F_2^1 THEN Output $y_k = C_{10}$.

The output is the weighted average of the y_k

$$y = \sum_{k=1}^{M} w_k \cdot y_k \tag{30}$$

where the weights w_k are computer as

$$w_k = \frac{\prod_{i=1}^{n} \mu_{F_i^k}(x_i)}{\sum_{j=1}^{M} \left[\prod_{i=1}^{n} \mu_{F_i^j}(x_i)\right]} \tag{31}$$

with $\sum_{i=1}^{M} w_i = 1$, and the μ's represent the membership functions.

C. Adaptive Fuzzy Strong Tracking Kalman Filter (AFSTKF)

As mentioned before, the process model of the KF is dependent on the dynamical characteristics of the vehicle onto which the navigation system is placed. The FLAS is employed to make the necessary tradeoff between accuracy and computational burden due to the increased dimension of the state vector and associated matrices. The FLAS was used to adapt the gain and, therefore, prevent the Kalman filter from divergence. It is widely known that a poorly designed mathematical model for the EKF may lead to the divergence. Clearly, if the plant parameters are subject to perturbations and dynamics of the system are too complex to be characterized by an explicit mathematical model, an adaptive scheme is needed. When the FLAS is employed, the lower order state model can be used without significantly compromising accuracy. In other words, for a given accuracy, the fuzzy adaptive Kalman filter is allowed to use a lower order state model. When a designer lacks sufficient information to develop a complete model or the parameters slowly change with time, the fuzzy system can be used to adjust the performance of EKF online, and it will remain sensitive to parameter variations by "remembering" the most recent data samples.

The covariance matrix of the innovation is given by [4], [5]

$$\mathbf{C}_{\upsilon_k} = E\left[\boldsymbol{\upsilon}_k \boldsymbol{\upsilon}_k^{\mathrm{T}}\right] = \mathbf{H}_k \mathbf{P}_k^{-} \mathbf{H}_k^{\mathrm{T}} + \mathbf{R}_k. \tag{32}$$

The trace of innovation covariance matrix can be obtained through the relation

$$\boldsymbol{\upsilon}_k^{\mathrm{T}} \boldsymbol{\upsilon}_k = \mathrm{tr}\left(\boldsymbol{\upsilon}_k \boldsymbol{\upsilon}_k^{\mathrm{T}}\right). \tag{33}$$

The DOD parameters for identifying the degree of change in vehicle dynamics can be determined based on the idea of (32) and (33). Examples for possible approaches are given as follows.

1) Category 1: The innovation information at the present epoch is employed to reflect the timely change in vehicle dynamics. The DOD parameter ξ can be defined as the trace of innovation covariance matrix at present epoch (i.e., the window size is one) divided by the number of satellites employed for navigation processing

$$\xi = \frac{\boldsymbol{\upsilon}_k^{\mathrm{T}}\boldsymbol{\upsilon}_k}{m} \tag{34}$$

where $\boldsymbol{\upsilon}_k = [\upsilon_1 \quad \upsilon_2 \quad \cdots \quad \upsilon_m]^T, m$ is the number of measurements (number of satellites). Alternatively, the averaged magnitude (absolute value) of innovation at the present epoch can also be used

$$\zeta = \frac{1}{m}\sum_{i=1}^{m}|\upsilon_i|. \tag{35}$$

2) Category 2: The discrepancy for the trace of innovation covariance matrix between the present (actual) and theoretical value is used. The DOD parameter can be of the form

$$\eta = \frac{\boldsymbol{\upsilon}_k^{\mathrm{T}}\boldsymbol{\upsilon}_k - \mathrm{tr}\left(\mathbf{H}_k\mathbf{P}_k^-\mathbf{H}_k^{\mathrm{T}} + \mathbf{R}_k\right)}{m} \tag{36a}$$

or

$$\eta = \frac{\left|\boldsymbol{\upsilon}_k^{\mathrm{T}}\boldsymbol{\upsilon}_k - \mathrm{tr}\left(\mathbf{H}_k\mathbf{P}_k^-\mathbf{H}_k^{\mathrm{T}} + \mathbf{R}_k\right)\right|}{m}. \tag{36b}$$

The alternative form is the rate for the trace of innovation covariance matrix for the current and theoretical value, given by

$$\mu = \frac{\boldsymbol{\upsilon}_k^{\mathrm{T}}\boldsymbol{\upsilon}_k}{\mathrm{tr}\left(\mathbf{H}_k\mathbf{P}_k^-\mathbf{H}_k^{\mathrm{T}} + \mathbf{R}_k\right)} \tag{37a}$$

or

$$\mu = \left|\frac{\boldsymbol{\upsilon}_k^{\mathrm{T}}\boldsymbol{\upsilon}_k}{\mathrm{tr}\left(\mathbf{H}_k\mathbf{P}_k^-\mathbf{H}_k^{\mathrm{T}} + \mathbf{R}_k\right)} - 1\right|. \tag{37b}$$

For each of the proposed approaches, only one scalar value needs to be determined and, therefore, the fuzzy rules can be simplified resulting in the decrease of computational efficiency.

In the FLAS, the DOD parameters are employed as the inputs for the fuzzy inference engines. By monitoring the DOD parameters, the FLAS is able to tune online the softening factor according to the fuzzy rules. For this reason, this scheme can adjust the fading factors adaptively and, therefore, improves estimation performance. When the softening factor is smaller, the tracking capability of STKF is better; while the softening factor is larger, the tracking accuracy of STKF is improved.

Fig. 4 provides the flow chart of the AFSTKF. The flow chart essentially contains three portions. Two blocks are indicated by the dashed line: the block on the left-hand side is the strong tracking loop; the block on the right-hand side is the FLAS for tuning the softening factor β. The portion that excludes the two blocks is essentially the standard EKF. The AFSTKF is employed to tune the softening factor according to the innovation information, and has the advantage over both EKF as well as STKF, in terms of both tacking capability and estimation accuracy.

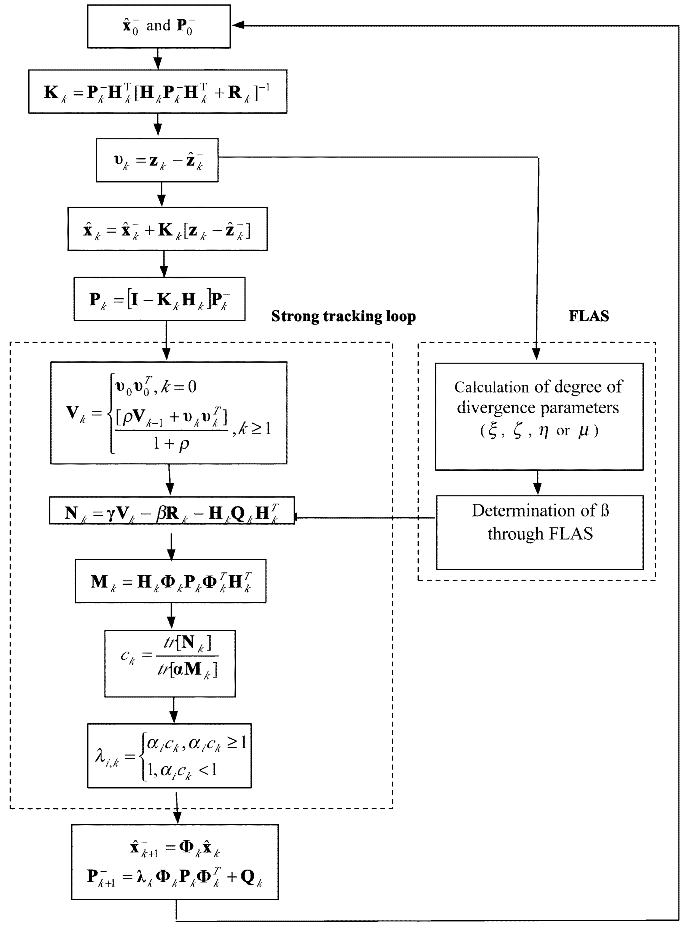

Fig. 4. Flow chart of the AFSTKF.

IV. SIMULATION EXPERIMENTS

Simulation experiments have been carried out to evaluate the performance of the AFSTKF approach in comparison with the conventional methods for GPS navigation processing. Simulation was conducted using a personal computer with Pentium 4 1.7 GHz CPU. The computer codes were developed by the authors using the Matlab 6.5 version software. The commercial software Satellite Navigation toolbox by GPSoft LLC was employed for generating the satellite positions and pseudoranges. Block diagram of the GPS navigation processing using the AFSTKF is shown in Fig. 5.

When selecting Kalman filtering as the navigation state estimator in the GPS receiver [2], [3], using b and d to represent the GPS receiver clock bias and drift, the differential equation for the clock error is written as

$$\begin{aligned} \dot{b} &= d + u_b \\ \dot{d} &= u_d \end{aligned} \tag{38}$$

where $u_b \sim N(0, S_f)$ and $u_d \sim N(0, S_g)$ are independent Gaussianly distributed white sequences. The dynamic process of the GPS receiver in a lower dynamic environment can be represented by the PV (Position-Velocity) model [2]. In such a case, we consider the GPS navigation filter with three position states, three velocity states, and two clock states, so that the state

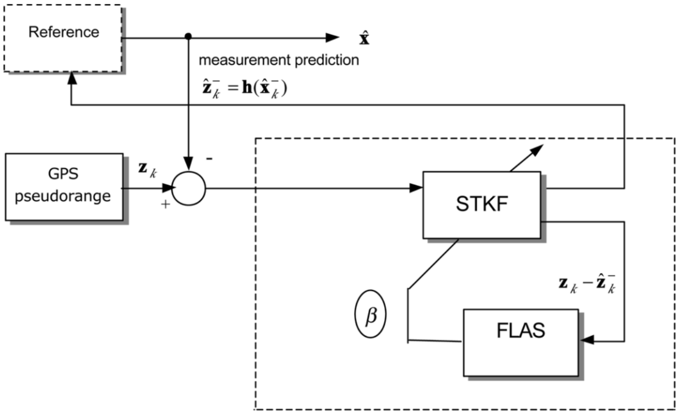

Fig. 5. GPS navigation processing using the AFSTKF.

to be estimated is a 8×1 vector. The process model governed by (9a) leads to

$$\begin{bmatrix} \dot{x}_1 \\ \dot{x}_2 \\ \dot{x}_3 \\ \dot{x}_4 \\ \dot{x}_5 \\ \dot{x}_6 \\ \dot{x}_7 \\ \dot{x}_8 \end{bmatrix} = \begin{bmatrix} 0 & 1 & 0 & 0 & 0 & 0 & 0 & 0 \\ 0 & 0 & 0 & 0 & 0 & 0 & 0 & 0 \\ 0 & 0 & 0 & 1 & 0 & 0 & 0 & 0 \\ 0 & 0 & 0 & 0 & 0 & 0 & 0 & 0 \\ 0 & 0 & 0 & 0 & 0 & 1 & 0 & 0 \\ 0 & 0 & 0 & 0 & 0 & 0 & 0 & 0 \\ 0 & 0 & 0 & 0 & 0 & 0 & 0 & 1 \\ 0 & 0 & 0 & 0 & 0 & 0 & 0 & 0 \end{bmatrix} \begin{bmatrix} x_1 \\ x_2 \\ x_3 \\ x_4 \\ x_5 \\ x_6 \\ x_7 \\ x_8 \end{bmatrix} + \begin{bmatrix} 0 \\ u_2 \\ 0 \\ u_4 \\ 0 \\ u_6 \\ u_7 \\ u_8 \end{bmatrix}$$

where x_1, x_3, x_5 represent the east, north, and vertical position; x_2, x_4, x_6 represent the east, north, and vertical velocity; and x_7 and x_8 represent the receiver clock offset and drift errors, respectively. The state transition matrix for the model can be found to be

$$\mathbf{\Phi}_k = \begin{bmatrix} 1 & \Delta t & 0 & 0 & 0 & 0 & 0 & 0 \\ 0 & 1 & 0 & 0 & 0 & 0 & 0 & 0 \\ 0 & 0 & 1 & \Delta t & 0 & 0 & 0 & 0 \\ 0 & 0 & 0 & 1 & 0 & 0 & 0 & 0 \\ 0 & 0 & 0 & 0 & 1 & \Delta t & 0 & 0 \\ 0 & 0 & 0 & 0 & 0 & 1 & 0 & 0 \\ 0 & 0 & 0 & 0 & 0 & 0 & 1 & \Delta t \\ 0 & 0 & 0 & 0 & 0 & 0 & 0 & 1 \end{bmatrix} \tag{39}$$

The process noise covariance matrix is shown in (40) at the bottom of the page. If only the pseudorange observables are available, the linearized measurement equation based on n observables can be written as given by

$$\underbrace{\begin{bmatrix} \rho_1 \\ \rho_2 \\ \vdots \\ \rho_n \end{bmatrix} - \begin{bmatrix} \hat{\rho}_1 \\ \hat{\rho}_2 \\ \vdots \\ \hat{\rho}_n \end{bmatrix}}_{\mathbf{Z_k}}$$

$$= \underbrace{\begin{bmatrix} h_x^{(1)} & 0 & h_y^{(1)} & 0 & h_z^{(1)} & 0 & 1 & 0 \\ h_x^{(2)} & 0 & h_y^{(2)} & 0 & h_z^{(2)} & 0 & 1 & 0 \\ \vdots & \vdots & \vdots & \vdots & \vdots & \vdots & \vdots & \vdots \\ h_x^{(n)} & 0 & h_y^{(n)} & 0 & h_z^{(n)} & 0 & 1 & 0 \end{bmatrix}}_{\mathbf{H_k}} \begin{bmatrix} x_1 \\ x_2 \\ x_3 \\ x_4 \\ x_5 \\ x_6 \\ x_7 \\ x_8 \end{bmatrix} + \begin{bmatrix} v_{\rho_1} \\ v_{\rho_2} \\ \vdots \\ v_{\rho_n} \end{bmatrix} \tag{41}$$

where the elements of the measurement model $\mathbf{H}_k$ are the partial derivatives of the predicted measurements with respect to each state, which is an $(n \times 8)$ matrix. Assuming measurement errors among satellites are uncorrelated, we have

$$\mathbf{R}_k = \begin{bmatrix} r_{\rho_1} & & & \mathbf{0} \\ & r_{\rho_2} & & \\ & & \ddots & \\ \mathbf{0} & & & r_{\rho_n} \end{bmatrix}. \tag{42}$$

Since we assumed that the differential GPS (DGPS) mode is used and most of the errors can be corrected, but the multipath and receiver measurement thermal noise cannot be eliminated. The measurement noise variances r_{ρ_i} value are assumed *a priori* known, which is set as 9 m^2. Let each of the white noise spectral amplitudes that drive the random walk position states be $S_p = 1.0(m/\sec^2)/\mathrm{rad}/\sec$. Also, let the clock model spectral amplitudes be $S_f = 0.4(10^{-18})\sec$ and $S_g = 1.58(10^{-18})\sec^{-1}$. These spectral amplitudes can be used to find the $\mathbf{Q}_k$ parameters in (40).

The simulation scenario is as follows. The experiment was conducted on a simulated vehicle trajectory originating from the position of North 25.1492° and East 121.7775° at an altitude of 100 m. This is equivalent to $[-3042329.2 \quad 4911080.2 \quad 2694074.3]^{\mathrm{T}}$ m in the WGS-84 ECEF coordinate system. The location of the origin is defined

$$\mathbf{Q}_k = \begin{bmatrix} S_p\frac{\Delta t^3}{3} & S_p\frac{\Delta t^2}{2} & & & & & & \\ S_p\frac{\Delta t^2}{2} & S_p\Delta t & & & & \mathbf{0} & & \\ & & S_p\frac{\Delta t^3}{3} & S_p\frac{\Delta t^2}{2} & & & & \\ & & S_p\frac{\Delta t^2}{2} & S_p\Delta t & & & & \\ & & & & S_p\frac{\Delta t^3}{3} & S_p\frac{\Delta t^2}{2} & & \\ & & & & S_p\frac{\Delta t^2}{2} & S_p\Delta t & & \\ & \mathbf{0} & & & & & S_f\Delta t + S_g\frac{\Delta t^3}{3} & S_g\frac{\Delta t^2}{2} \\ & & & & & & S_g\frac{\Delta t^2}{2} & S_g\Delta t \end{bmatrix} \tag{40}$$

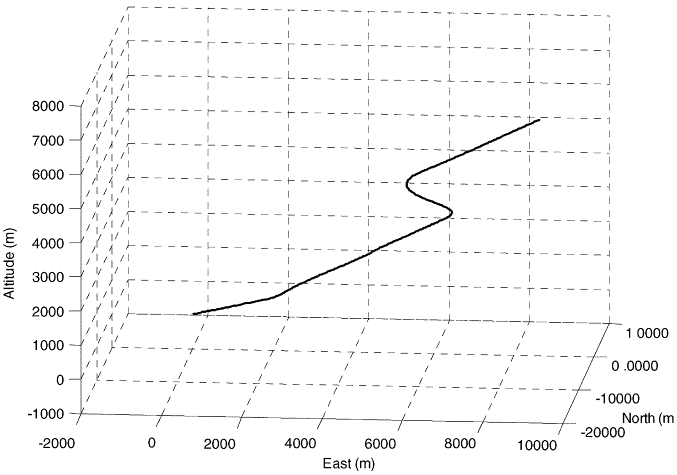

Fig. 6. Three-dimensional vehicle trajectory.

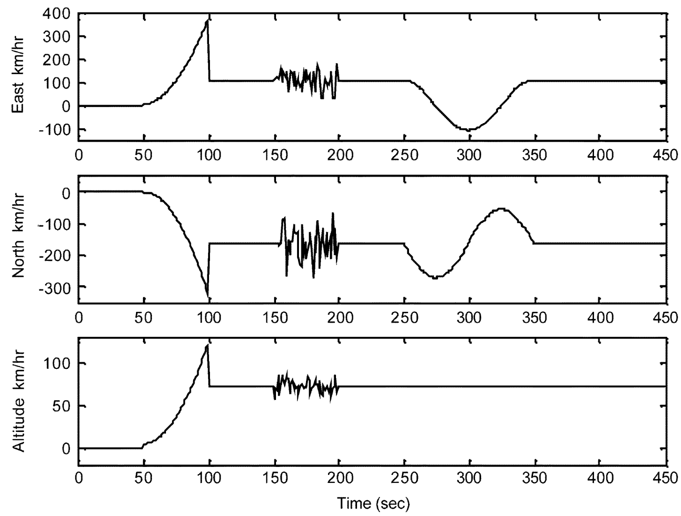

Fig. 7. Vehicle velocity in the east, north, and vertical components.

TABLE I
DESCRIPTION OF VEHICLE MOTION

Time interval (sec)	Motion
[0-50]	Stationary
[51-100]	Constant acceleration
[101-150]	Constant velocity
[151-200]	Variable acceleration
[201-250]	Constant velocity
[251-350]	Circular motion, clockwise turn
[351-450]	Constant velocity

TABLE II
SETTING OF PARAMETERS FOR EKF, STKF, AND AFSTKF

	EKF	STKF	AFSTKF
r_{ρ_i}	$9m^2$	$9m^2$	$9m^2$
dt	0.15 sec	0.15 sec	0.15 sec
S_p	$1.0(m/\sec^2)/rad/\sec$	$1.0(m/\sec^2)/rad/\sec$	$1.0(m/\sec^2)/rad/\sec$
S_g	$1.58(10^{-18})\sec^{-1}$	$1.58(10^{-18})\sec^{-1}$	$1.58(10^{-18})\sec^{-1}$
S_f	$0.4(10^{-18})\sec$	$0.4(10^{-18})\sec$	$0.4(10^{-18})\sec$
β	NA	4.5	FLAS outputs
ρ	NA	0.95	0.95
a_i	NA	1	1

as the $(0, 0, 0)$ m location in the local tangent East-North-Up (ENU) frame. The three-dimensional plot of trajectory is shown in Fig. 6. The description of the vehicle motion is listed in Table I. In addition, vehicle velocity in the east, north, and vertical components are also provided in Fig. 7 for providing better insight into vehicle dynamic information in each time interval. The related setting of parameters for the EKF, STKF, and AFSTKF is listed in Table II.

The parameter β in STKF is a constant and does not change subject to the change in dynamics. When the vehicle is in high dynamic environments, a smaller softening factor (β) will be required for better tracking capability; when the vehicle is in lower dynamic environments, a larger β will be needed for better estimation precision. Therefore, the improved version of STKF, which incorporates the FLAS, can be introduced for automatically adjust the value of β. For the vehicle in a very low dynamic environment, β should be increased to a very large value, which leads $\lambda_{i,k}$ to 1 and results in the standard Kalman filter.

The philosophy for defining the rules is straightforward: 1) for the case that the DOD parameter is small, our objective is to obtain results with better estimation accuracy, and a larger softening factor (β) should be applied and 2) for the case that the DOD parameter is increased, our objective is to increase the tracking capability, and a smaller softening factor should be applied. The membership functions (MFs) of input fuzzy variable DOD parameters as shown in Figs. 8–11 are triangle MFs, obtained by the function

$$\mu(x) = \begin{cases} 0, & x \leqslant a \\ \frac{x-a}{b-a}, & a \leqslant x \leqslant b \\ \frac{c-x}{c-b}, & b \leqslant x \leqslant c \\ 0, & c \leqslant x \end{cases}.$$

The first-order T-S model is suggested. The zero-order model needs more complicated MFs and rule base and is, therefore, more difficult to determine. The presented FLAS is the *If-Then* form and consists of three rules. Four methods corresponding to four DOD parameters are presented.

1) Method 1—use ξ in (34) as the DOD parameter
   a) IF ξ is zero THEN β is $\xi + 10$
   b) IF ξ is small THEN β is $\xi + 4$
   c) IF ξ is large THEN β is 1

   The membership functions of input fuzzy variable ξ are provided in Fig. 8.
2) Method 2—use ζ in (35) as the DOD parameter
   a) IF ζ is zero THEN β is $3\zeta + 8$
   b) IF ζ is small THEN β is $2\zeta + 4$
   c) IF ζ is large THEN β is 1

   The membership functions of input fuzzy variable ζ are provided in Fig. 9.

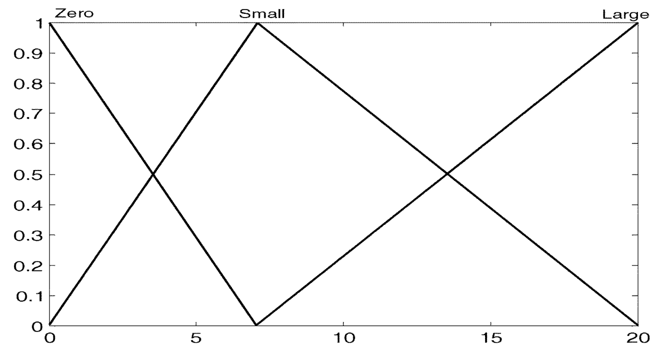

Fig. 8. Membership functions of input fuzzy variable ξ.

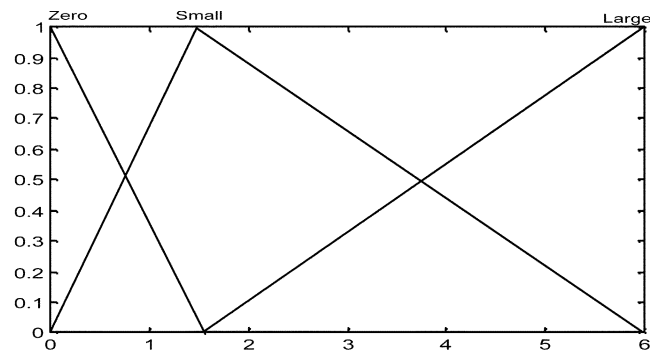

Fig. 9. Membership functions of input fuzzy variable ζ.

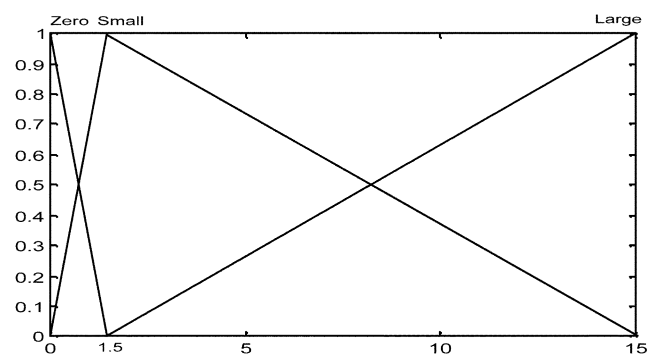

Fig. 10. Membership functions of input fuzzy variable η.

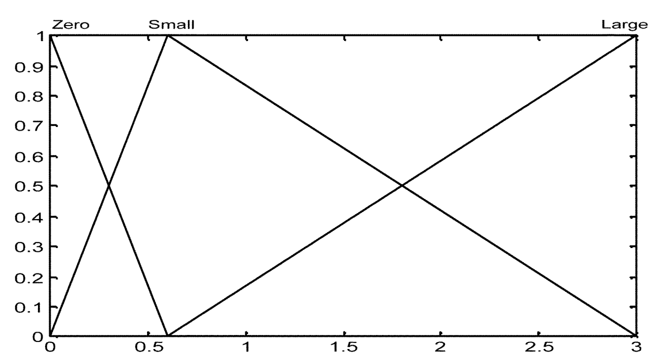

Fig. 11. Membership functions of input fuzzy variable μ.

3) Method 3—use η in (36b) as the DOD parameter
   a) IF η is zero THEN β is $2\eta + 10$
   b) IF η is small THEN β is $\eta + 7$
   c) IF η is large THEN β is 1

   The membership functions of input fuzzy variable η are provided in Fig. 10.

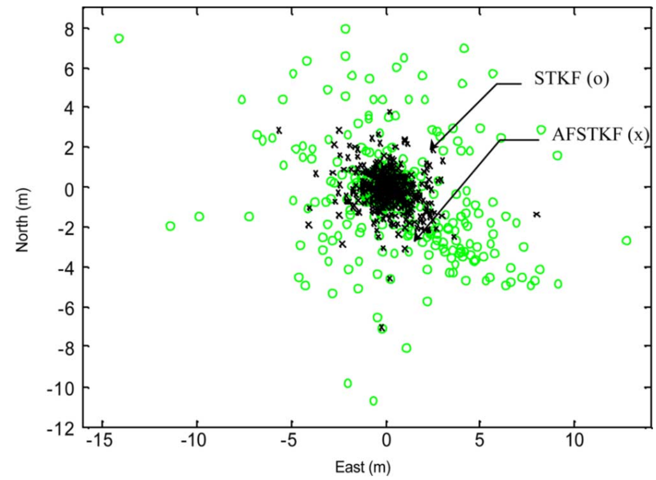

Fig. 12. Comparison of GPS positioning errors. (1) STKF (o). (2) AFSTKF (x).

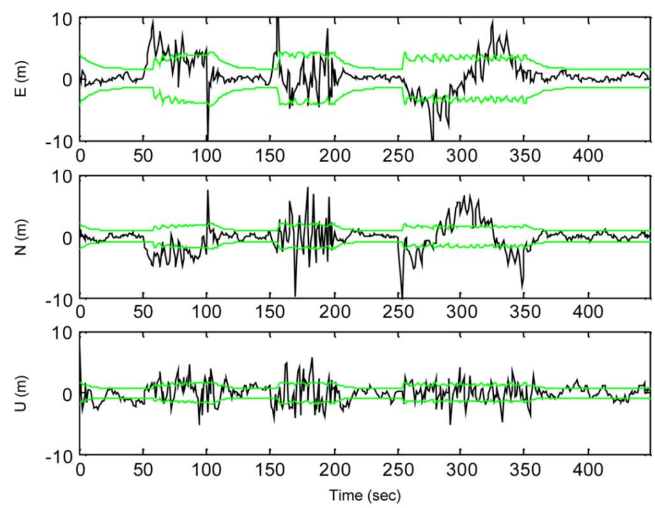

(a)

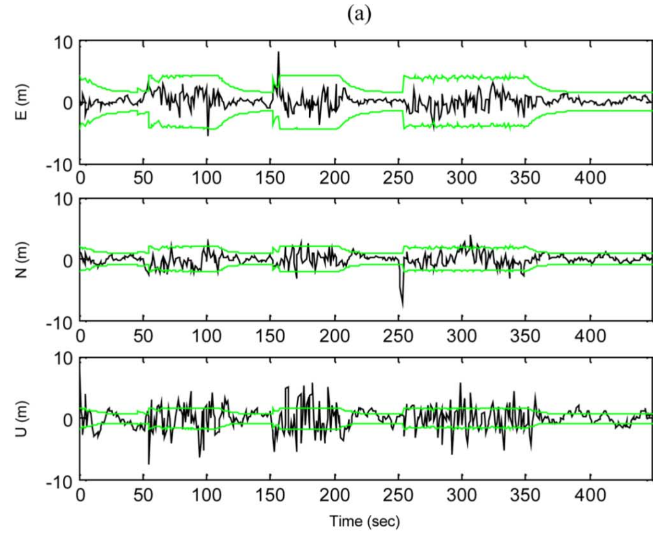

(b)

Fig. 13. East, north, and up components of the navigation results and the corresponding 1-σ bound based on the STKF method and AFSTKF method. (a) STKF. (b) AFSTKF.

4) Method 4—use μin (37b) as the DOD parameter
   a) IF $\mu$is zero THEN β is $2\mu + 20$
   b) IF μ is small THEN β is $\mu + 10$
   c) IF $\mu$is large THEN β is 2

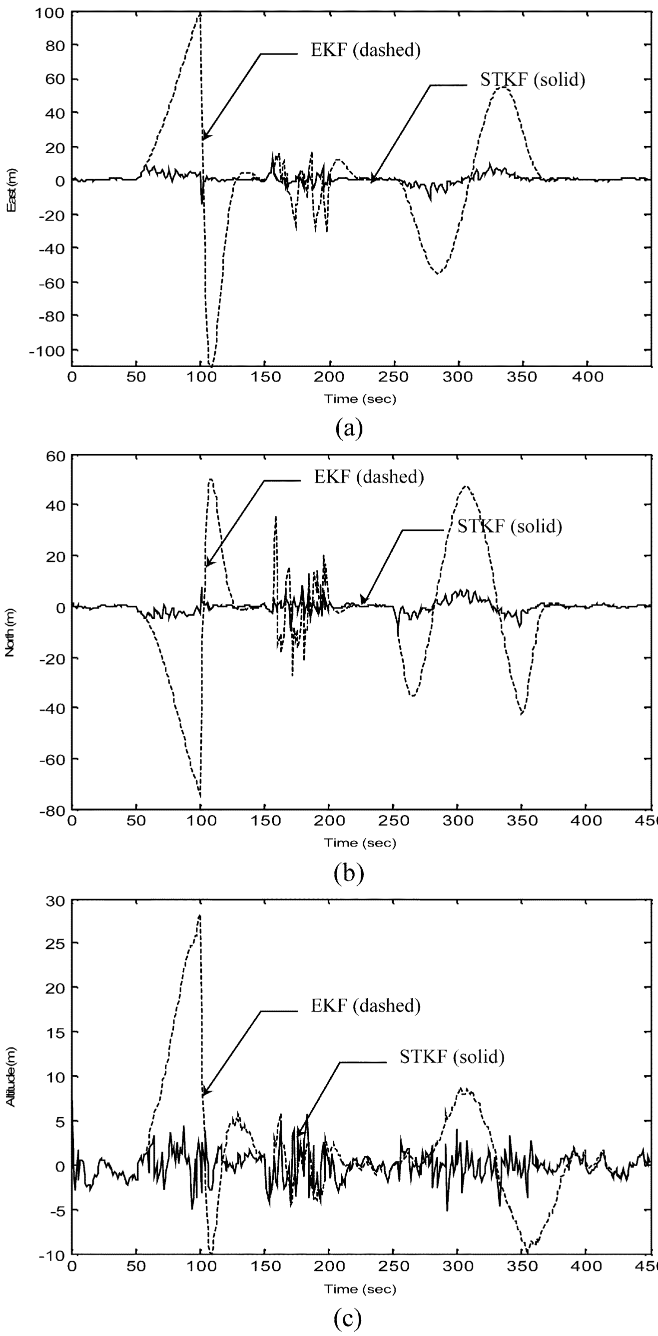

Fig. 14. Navigation accuracy comparison for STKF and EKF. (a) East. (b) North. (c) Altitude.

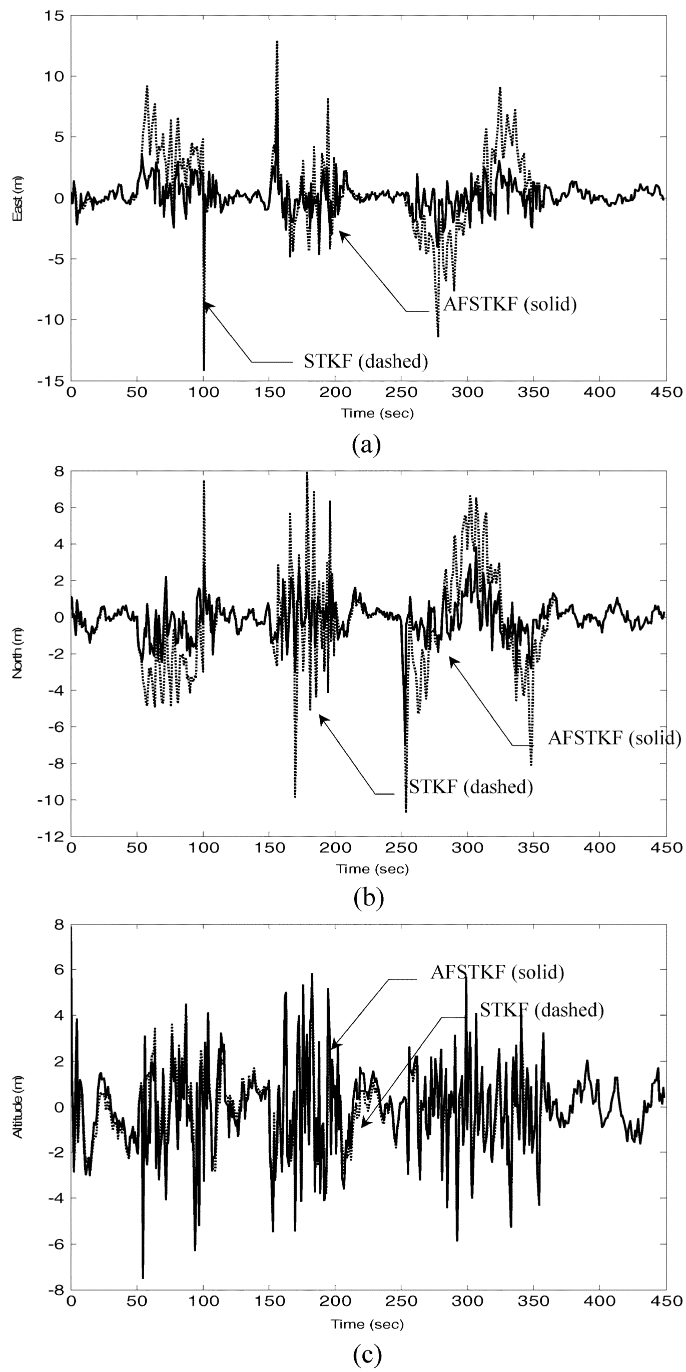

Fig. 15. Navigation accuracy comparison for AFSTKF and STKF. (a) East. (b) North. (c) Altitude.

The membership functions of input fuzzy variable $\mu$are provided in Fig. 11.

Figs. 12–17 provide the GPS navigation results for the standard EKF, STKF, and AFSTKF approaches. For comparison purposes, various types of illustrations are provided and discussed as follows. The navigational errors in the East–North plane for the AFSTKF method and the STKF method is given in Fig. 12. Subplot (a) and (b), respectively, of Fig. 13 show the East, North, and Vertical components of navigational errors and the corresponding 1-σ bounds for the STKF and the AFSTKF, respectively. Performance comparison between STKF and EKF is shown in Fig. 14; performance comparison between AFSTKF and STKF is shown in Fig. 15. Figs. 16 and 17 provide the error standard deviation traces of east-component position errors for STKF versus EKF, and for AFSTKF versus STKF, respectively.

It can be seen that substantial estimation accuracy improvement is obtained by using the proposed technique, discussed as follows.

1) In the time interval of 0–50 s, the vehicle is stationary. For this case, EKF, STKF, and AFSTKF all provide good results. At this time interval, the DOD is small. At this moment, the FLAS gives a larger softening factor β resulting in better smoothness.

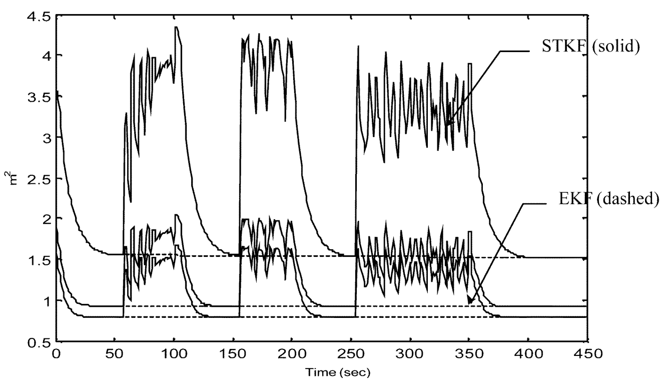

Fig. 16. Comparison of error standard deviation traces for STKF and EKF.

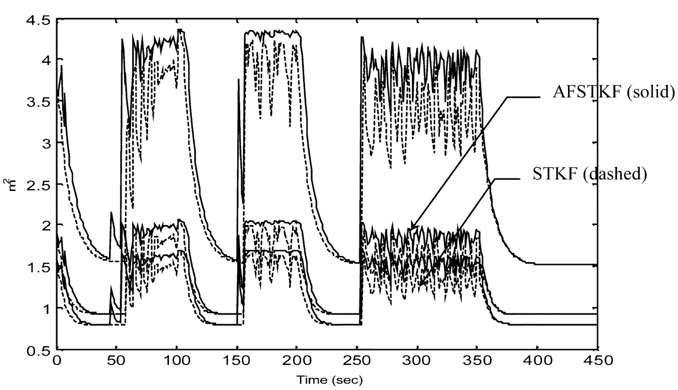

Fig. 17. Comparison of error standard deviation traces for AFSTKF and STKF.

2) In the three time intervals, 101–150, 201–250, and 351–450 s, the vehicle is not maneuvering and is conducting constant-velocity straight-line motion for all the three components. By using T-S fuzzy logic, the FLAS senses smaller values of DOD parameters, and gives a larger softening factor resulting in more precise results. It is clearly seen that the AFSTKF demonstrates very good adaptation property. With large softening factors, the fading factor is approaching 1, and both the AFSTKF and STKF deteriorate to the standard EKF. As a result, the navigation accuracies based on the EKF, STKF, and AFSTKF are equivalent.
3) In the three time intervals, 51–100, 151–200, and 251–350 s, the vehicle is maneuvering. The mismatch of the model leads the conventional EKF to a large navigation error, while the FLAS timely detects the increase of DOD parameter, and then reduces the softening factor so as to maintain good tracking capability. It is verified that, by monitoring the innovation information, the AFSTKF has the good capability to detect the change in vehicle dynamics and adjust the softening factor for preventing the divergence and having better navigation accuracy.

In addition, the FLAS in the AFSTKF automatically adjust the softening factor (β) based on the timely innovation information. The softening factors determined by the FLAS, and the corresponding fading factors are given in Fig. 18. It can be seen that when the vehicle is in high dynamic environment, β will be tuned to a smaller value; in a low dynamic case, β will be tuned to a very larger value. The case that β is very large will lead the fading factor $\lambda_{i,k}$ to 1, and the AFSTKF becomes the standard EKF. The fact, as was predicted, can be seen in the time intervals 0–50, 101–150, 201–250, and 351–405 s.

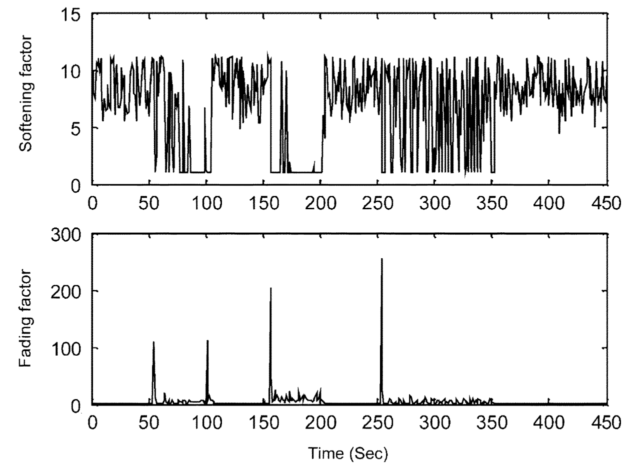

Fig. 18. The softening factors (top) and fading factors (bottom).

V. Conclusion

The conventional EKF requires more states for better navigation accuracy and does not present the capability to monitor the change of parameters due to changes in vehicle dynamics. Traditional STKF approach for determining the softening factors heavily relies on personal experience or computer simulation using a heuristic searching scheme. This paper has presented an AFSTKF for GPS navigation processing to prevent the divergence problem in high dynamic environments.

Through the use of fuzzy logic, the FLAS in the AFSTKF has been employed as a mechanism for timely detecting the dynamical changes and implementing the online tuning of the softening factor by monitoring the innovation information to maintain good tracking capability. When a designer does not have sufficient information to develop the complete filter models or when the filter parameters are slowly changing with time, the fuzzy system can be employed to enhance the STKF performance. By using FLAS, the lower order of the filter model can be utilized and, therefore, less computational effort will be sufficient without compromising estimation accuracy significantly. The navigation accuracy based on the proposed method has been compared with the STKF and EKF and has demonstrated substantial improvement in both navigational accuracy and tracking capability.

Acknowledgment

Valuable suggestions and detailed comments by the reviewers are gratefully acknowledged.

References

[1] A. Gelb, *Applied Optimal Estimation*. Cambridge, MA: MIT Press, 1974.
[2] R. G. Brown and P. Y. C. Hwang, *Introduction to Random Signals and Applied Kalman Filtering*, 3rd ed. New York: Wiley, 1997.

[3] P. Axelrad and R. G. Brown, *GPS Navigation Algorithms*, B. W. Parkinson, J. J. Spilker, P. Axelrad, and P. Enga, Eds. Washington, DC: AIAA, 1996, vol. I, Global Positioning System: Theory and Applications, ch. 9.

[4] R. K. Mehra, "Approaches to adaptive filtering," *IEEE Trans. Autom. Control*, vol. AC-17, pp. 693–698, 1972.

[5] A. H. Mohamed and K. P. Schwarz, "Adaptive Kalman filtering for INS/GPS," *J. Geodesy*, vol. 73, no. 4, pp. 193–203, 1999.

[6] D. H. Zhou and P. M. Frank, "Strong tracking Kalman filtering of nonlinear time-varying stochastic systems with coloured noise: Application to parameter estimation and empirical robustness analysis," *Int. J. Control*, vol. 65, no. 2, pp. 295–307, 1996.

[7] X. Deng, W. Guo, J. Xie, and J. Liu, "Particle filter based on strong tracking filter," in *Proc. 4th Int. Conf. Mach. Learning Cybern.*, Guangzhou, 2005, pp. 658–661.

[8] T. Takagi and M. Sugeno, "Fuzzy identification of systems and its application to modelling and control," *IEEE Trans. Syst., Man, Cybern.*, vol. SMC-15, no. 1, pp. 116–132, 1985.

[9] J. Z. Sasiadek, Q. Wang, and M. B. Zeremba, "Fuzzy adaptive Kalman filtering for INS/GPS data fusion," in *Proc. 15th IEEE Int. Symp. Intell. Control,* , Rio, Patras, Greece, 2000, pp. 181–186.

[10] G. Abdelnour, S. Chand, and S. Chiu, "Applying fuzzy logic to the Kalman filter divergence problem," in *Proc. IEEE Int. Conf. Syst., Man, Cybern.*, Le Touquet, France, 1993, pp. 630–634.

[11] K. Kobayashi, K. Cheok, and K. Watanabe, "Estimation of the absolute vehicle speed using fuzzy logic rule-based Kalman filter," in *Proc. Amer. Control Conf.*, Seattle, 1995, pp. 3086–3090.

[12] K. Mostov and A. Soloviev, "Fuzzy adaptive stabilization of higher order Kalman filters in application to precision kinematic GPS," in *Proc. ION GPS*, Kansas City, 1996, vol. 2, pp. 1451–1456.

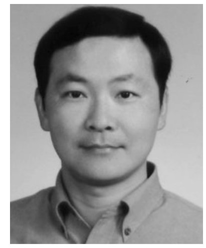

Dah-Jing Jwo was born in Taiwan, in February 1964. He received the Ph.D. degree in aerospace engineering from the University of Texas at Arlington, Arlington, TX, in 1995.

From 1997 to 1998, he worked in industry and the Center for Aviation and Space Technology at the Industrial Technology Research Institute (ITRI), Hsinchu, Taiwan. In 1998, he joined the faculty of National Taiwan Ocean University, where he is currently an Associate Professor and Chairman with the Department of Communications and Guidance Engineering. His current research interests include GPS navigation, multisensor integrated navigation, estimation theory and applications, artificial intelligence and vehicle guidance, navigation, and control (GN&C) design.

Sheng-Hung Wang was born in Taiwan, in March 1980. He received the B.S. degree in aerospace engineering from Tamkang University, Taipei, Taiwan, in 2004, and the M.S. degree in communications and guidance engineering from National Taiwan Ocean University, Keelung, Taiwan, in 2006.

His research interests include GPS navigation, artificial intelligence, and the unmanned aerial vehicle (UAV) design.